Conformational Dynamics of Free and Catalytically Active Thermolysin Are Indistinguishable by Hydrogen/Deuterium Exchange Mass Spectrometry[†]

Yu-Hong Liu and Lars Konermann*

Department of Chemistry, The University of Western Ontario, London, Ontario N6A 5B7, Canada

Received March 18, 2008; Revised Manuscript Received April 24, 2008

ABSTRACT: Conformational dynamics are thought to be a prerequisite for the catalytic activity of enzymes. However, the exact relationship between structural fluctuations and function is not well understood. In this work hydrogen/deuterium exchange (HDX) and electrospray ionization mass spectrometry (ESI-MS) are used for exploring the conformational dynamics of thermolysin. Amide HDX reflects the internal mobility of proteins; regions that undergo frequent unfolding−refolding show faster exchange than segments that are highly stable. Thermolysin is a zinc protease with an active site that is located between two lobes. Substrate turnover is associated with hinge bending that leads to a closed conformation. Product release regenerates the open form, such that steady-state catalysis involves a continuous closing/opening cycle. HDX/ESI-MS with proteolytic peptide mapping in the absence of substrate shows that elements in the periphery of the two lobes are most mobile. A comparison with previous X-ray data suggests that these peripheral regions undergo quite pronounced structural changes during the catalytic cycle. In contrast, active site residues exhibit only a moderate degree of backbone flexibility, and the central zinc appears to be in a fairly rigid environment. The presence of both rigid and moderately flexible elements in the active site may reflect a carefully tuned balance that is required for function. Interestingly, the HDX behavior of catalytically active thermolysin is indistinguishable from that of the free enzyme. This result is consistent with the view that catalytically relevant motions preexist in the resting state and that enzyme function can only be performed within the limitations given by the intrinsic dynamics of the protein. The data presented in this work indicate the prevalence of stochastic elements in the function of thermolysin, rather than supporting a deterministic mechanism.

It is widely accepted that conformational dynamics represent an integral part of enzymatic reaction mechanisms. X-ray crystallographic data for many enzymes reveal pronounced structural changes upon substrate (or inhibitor) binding. Typically, the substrate-free enzyme adopts an "open" conformation where the active site is relatively exposed. Conformational changes upon binding lead to a more "closed" structure where the substrate is shielded from the solvent and in contact with the catalytically active residues. Data of this kind imply that enzymes have to pass through a continuous cycle of closing/opening events as they catalyze a biochemical process. Although the role of conformational dynamics is most apparent for substrate binding and product release, structural plasticity is thought to perpetrate many other functional aspects as well (*1*–*6*). Increased protein flexibility has been linked to enhanced enzymatic activity in several cases (*7*–*10*), and a few studies suggest a direct correlation between the time scale of conformational fluctuations and the turnover number (*11*–*13*).

Two popular approaches for exploring the link between enzyme dynamics and function are NMR[1] spin relaxation experiments (*13, 14*) and amide hydrogen/deuterium exchange (HDX) studies by electrospray mass spectrometry (ESI-MS) (*8, 15*). The former technique is based on the equilibration of a perturbed spin system, a process that is mediated by stochastic fluctuations of the magnetic field at the nuclei of interest. These field fluctuations are linked to the internal motions of the protein (*16*). HDX/ESI-MS monitors the exchange kinetics of hydrogens along the polypeptide backbone. Most of these hydrogens are protected from exchange due to (i) the involvement in stable N−H···O═C hydrogen bonds and/or (ii) steric shielding from the solvent. HDX at these sites is mediated by thermally activated excursions to partially unfolded conformers, associated with the short-lived disruption of H-bonds and transient solvent access. Structural transitions of this kind occur on time scales ranging from picoseconds to seconds. They may correspond to local, subglobal, or global events (*17, 18*). In the commonly encountered EX2 regime every exchangeable site has to pass through numerous

[†] This work was supported by the Natural Sciences and Engineering Research Council of Canada (NSERC), the Canada Foundation for Innovation (CFI), and the Canada Research Chairs Program.

* To whom correspondence should be addressed. Telephone: (519) 661-2111 ext 86313. Fax: (519) 661-3022. E-mail: konerman@uwo.ca.

[1] Abbreviations: ESI-MS, electrospray ionization mass spectrometry; HDX, hydrogen/deuterium exchange; HEPES, 4-(2-hydroxyethyl)piperazine-1-ethanesulfonic acid; HPLC, high-performance liquid chromatography; LeuEnk, leucine enkephalin; NMR, nuclear magnetic resonance.

10.1021/bi800463q CCC: $40.75
Published on Web 05/22/2008

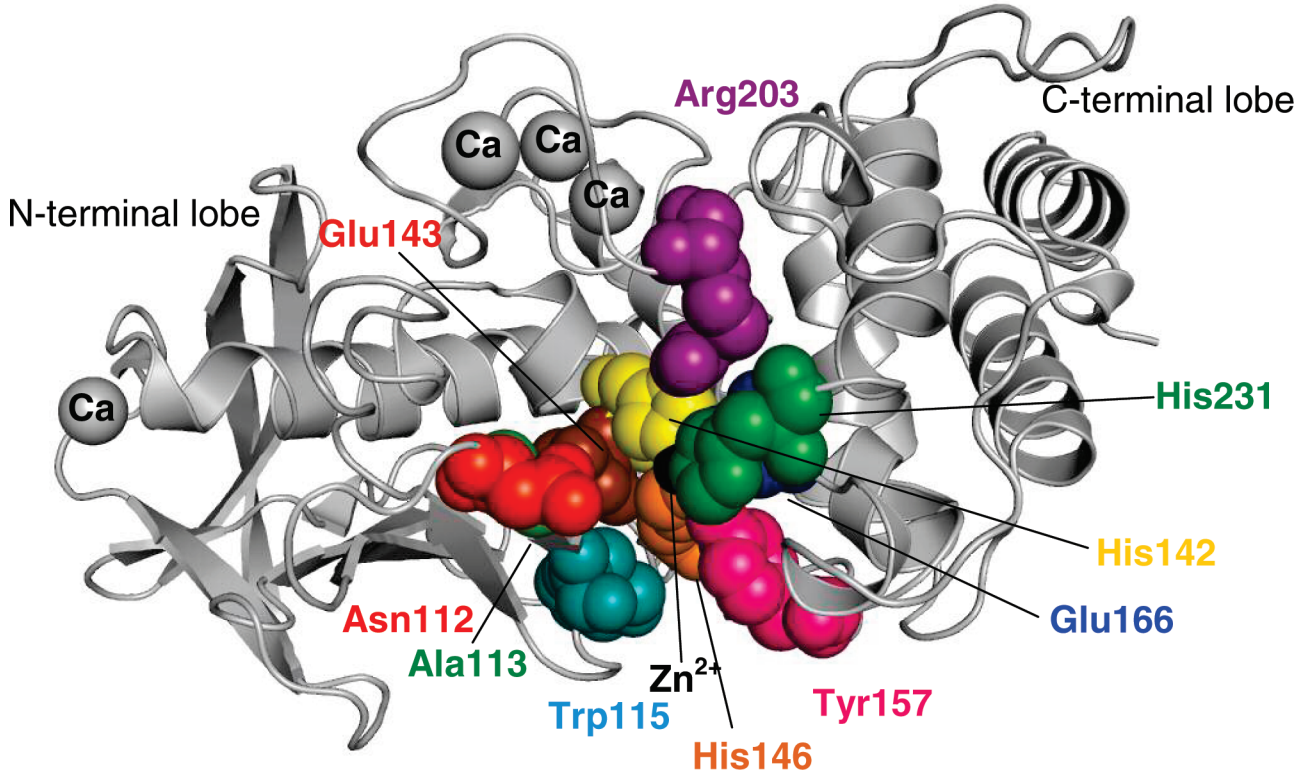

FIGURE 1: Structure of thermolysin (PDB code 8TLN) (*29*) with active site residues depicted in space-filling representation. The colors used for this figure are not related to the kinetic color coding employed throughout the rest of this work.

unfolding−refolding cycles before HDX occurs, because the exchange probability associated with every individual unfolding event is small (*19*). The deuteration pattern of a protein measured after a given exchange time reflects the added contributions of all these fluctuations. As a result, even transient conformers with small equilibrium populations can have profound effects on the HDX behavior (*20*). Highly flexible and solvent-exposed regions undergo more rapid exchange than rigid sections that are buried inside the protein core. Smith and co-workers (*21*) have pioneered the use of rapid acid quenching and cooling, followed by pepsin digestion and chromatographic analysis for monitoring deuteration patterns in a spatially resolved manner by ESI-MS (*22–26*).

Thermolysin [EC 3.4.24.27, molecular mass 34332 Da (excluding metals)] is a zinc endopeptidase from *Bacillus thermoproteolyticus* that has its pH optimum in the neutral range (*27*). It catalyzes the hydrolysis of peptide bonds on the N-terminal side of hydrophobic amino acid residues with low cleavage specificity. Four bound calcium ions are not involved in catalysis but serve to protect surface loops from autolysis and infer thermal stability (Figure 1) (*27*). The active site zinc has approximate tetrahedral coordination and is ligated by His142, His146, and Glu166. Water serves as the fourth ligand. The mechanism of peptide bond hydrolysis involves polarization of the substrate carbonyl by Zn^{2+}, thereby facilitating nucleophilic attack on the carbonyl carbon by the zinc-bound water. From the resulting tetrahedral intermediate the reaction proceeds to the fully hydrolyzed product state. Several other residues are involved in the catalytic process, including Asn112, Ala113, Trp115, Glu143, Tyr157, Arg203, and His231 (*27, 28*). The active site is located within a cleft that is formed between the two major lobes of the protein. The N-terminal lobe contains a central α-helix and several β-sheets, whereas the C-terminal domain predominantly adopts a helical secondary structure (*29*). The protein does not possess any disulfide bonds. Upon substrate binding the two lobes rotate relative to one another by 5.1°, thus exhibiting hinge-bending behavior similar to that previously observed for related proteases (*29, 30*).

It remains an open question in how far the conformational dynamics of enzymes are different during catalysis and in the substrate-free state. One possibility is that the presence of substrate directs structural fluctuations along a well-ordered sequence of conformational events, including large-scale transitions associated with binding and product release (*31*). The absence of substrate might alter the energy landscape in such a way that the same motions no longer occur. For example, a substrate-free protein could be trapped in an "open" conformation while still undergoing other types of thermal motions. Alternatively, an enzyme might sample catalytically relevant conformations both in the presence and in the absence of substrate, resulting in conformational dynamics that are almost indistinguishable for both cases. Several previous studies support the notion of a mobility enhancement during catalysis (*13, 32–35*), whereas others suggest that the internal motions of enzymes are very similar with and without substrate (*8, 10–12, 36–41*). The current work initially explores the conformational dynamics of catalytically inactive thermolysin. This is followed by comparative measurements in the presence and absence of the substrate leucine enkephalin (LeuEnk). It is found that deuterium incorporation under both conditions is indistinguishable, suggesting that the conformational dynamics of the protein are largely independent of the presence of substrate.

EXPERIMENTAL PROCEDURES

Materials. Thermolysin from *B. thermoproteolyticus*, porcine pepsin, insulin chain B, and human angiotensin I were obtained from Sigma (St. Louis, MO). LeuEnk and bradykinin were supplied by Bachem (King of Prussia, PA). Deuterium oxide was purchased from Cambridge Isotope Laboratories (Andover, MA), and ammonium-d_4 deuteroxide (25% in D_2O) was obtained from Isotec/Sigma-Aldrich. All chemicals were used without further purification. Thermolysin solutions and D_2O-based labeling buffers were adjusted to a pH meter reading of 7.4, with 40 mM HEPES, 10 mM $CaCl_2$ and 200 mM NaCl, unless noted otherwise. Autodigestion tests were carried out by measuring the ion intensity of the intact protein by ESI-MS for various incubation times. Notable signal loss was observed at 37 °C over 5 h. At temperatures of 22 °C and below there was no evidence of self-degradation during this period (data not shown).

HDX/ESI-MS. Substrate-free thermolysin in aqueous solution was mixed with 4 volumes of D_2O labeling buffer, resulting in a protein concentration of 50 μM. Aliquots (50 μL) were taken at various times ranging from 14 s to 5 h after initiation of labeling. These samples were quenched by mixing with 26 μL of 500 mM potassium phosphate for a final pH of 2.5, followed by flash freezing in liquid nitrogen and overnight storage at −80 °C. Pepsin digestion was carried out at pH 2.5 and 0 °C. The samples were quickly thawed and mixed with 46 μL of a 55 μM pepsin stock solution (in aqueous acetic acid, pH 4.1) for 1 min. The final thermolysin:pepsin molar ratio was 1:1, and the final thermolysin concentration was 20.5 μM. The resulting peptic fragments were desalted and separated within 12 min on an equilibrated reversed-phase column (Jupiter 4 μ Proteo, C12, 50 × 1 mm; Phenomenex, Torrance, CA) with an online prefilter (KrudKatcher; Phenomenex) coupled to a Waters 1525μ HPLC pump at a flow rate of 100 μL min^{-1}, using a water/acetonitrile gradient in the presence of 0.05% trifluoroacetic acid. The injection loop volume was 10 μL, and the total amount of protein loaded onto the column was 205 pmol. The column, accessories, injector, and extensively coiled solvent delivery lines were embedded in an ice bath to minimize back-exchange. The syringe used for injection was chilled on ice as well. Peptides were analyzed by ESI-MS on a Q-TOF Ultima (Waters, Milford, MA) with source and desolvation temperatures of 80 and 250 °C, respectively, and a cone voltage of 50 V. This procedure resulted in 41 peptic fragments that could be used for monitoring the HDX behavior of thermolysin. The identity of each peptide was confirmed by MS/MS based on the known thermolysin sequence (*42*) (see also Figure 2).

In separate control experiments three test peptides (bradykinin, angiotensin I, and insulin chain B) were used to estimate the extent of back-exchange associated with the method used. The peptides were exposed to a D_2O/H_2O mixture (80:20 v/v) for 22 h, after which labeling had gone to completion. Subsequently, the peptides were subjected to the same analysis procedure as thermolysin, except that the "digestion" step was simulated without pepsin. The resulting elution times were between 7 min (bradykinin) and 12 min (insulin chain B), thereby covering a range during which most thermolysin peptic fragments eluted. The average back-exchange for the three peptides was around 16%.

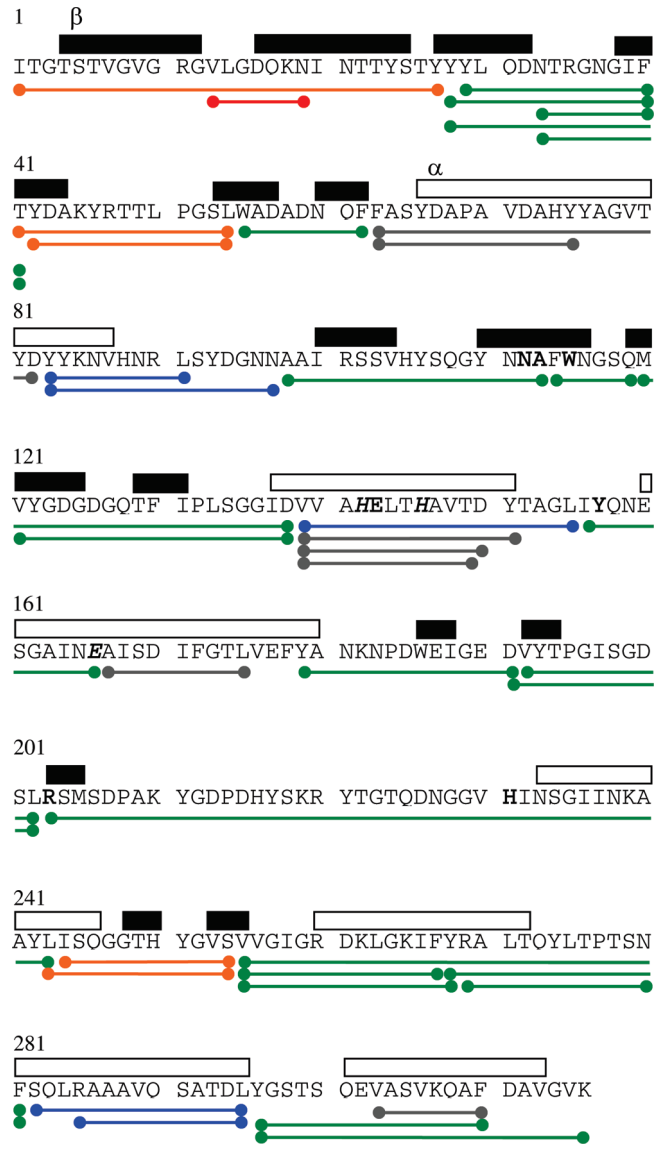

FIGURE 2: Thermolysin sequence with β-sheet and α-helical regions indicated in black and white, respectively (*29*). Solid lines indicate peptic fragments used for mapping the conformational dynamics by HDX/ESI-MS, with N- and C-termini marked as spheres. The color coding reflects the average HDX rate constant of individual peptides determined from Figure 6, i.e., gray (slowest), blue (slow), green (intermediate), orange (fast), and red (fastest). Active site residues are in bold; Zn^{2+} ligands are shown in bold italics.

Zero time point controls (m_0) for the correction of artifactual in-exchange were performed by exposing thermolysin to a mixture of D_2O and quenching buffer, using the solutions described above. Controls for fully exchanged thermolysin (m_{100}, for the correction of artifactual back-exchange) were prepared as follows: 50 μM thermolysin was incubated in 80% labeling buffer with 37.5 mM sodium hydroxide at 39 °C for 72 h. A 25 μL aliquot was quenched at pH 2.5 with 500 mM potassium phosphate containing 42 mM HCl and analyzed as described above. Biolynx 4.0 (Waters), HX-Express (*43*), and manual inspection were employed to analyze the mass m of all 41 peptic fragments as a function of labeling time. Percentage deuteration was determined as (*10*)

$$\% \text{ deuteration} = \frac{m - m_0}{m_{100} - m_0} \quad (1)$$

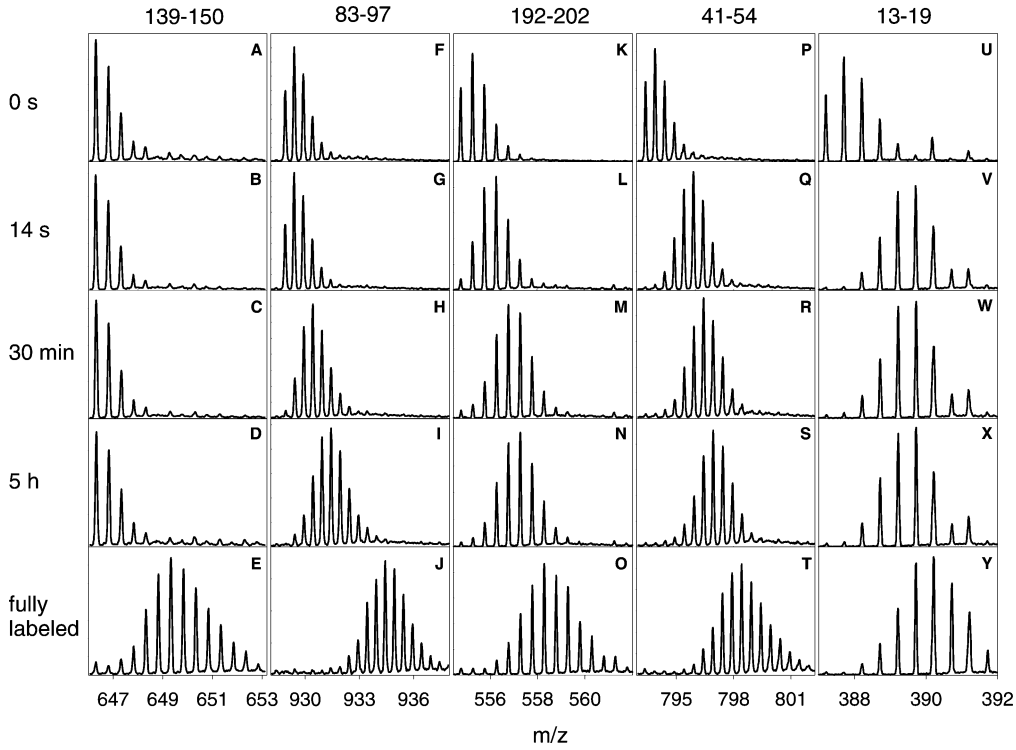

FIGURE 3: Partial ESI mass spectra, representing HDX data for five selected peptic fragments at labeling times of 14 s, 30 min, and 5 h. Also shown are the t_0 (top row) and fully labeled controls (bottom row). All signals shown correspond to doubly charged $[M + 2H]^{2+}$ peptide ions. The data were recorded at 22 °C in the absence of substrate.

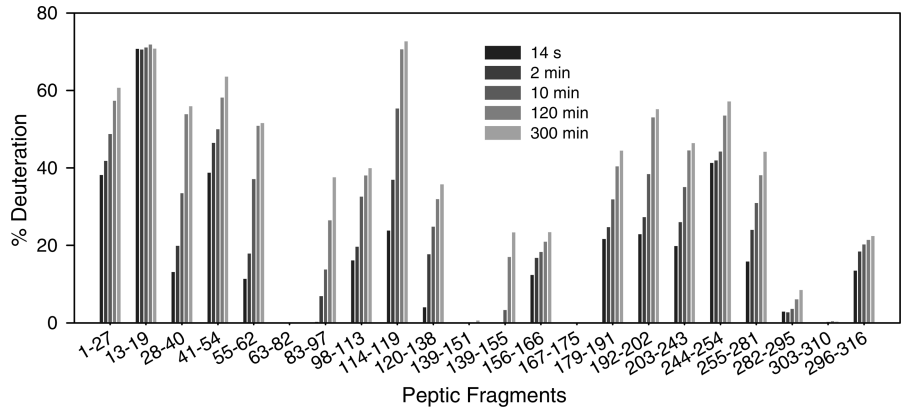

FIGURE 4: Deuteration levels at five different labeling times for 22 peptides that cover almost the entire thermolysin sequence. The data were recorded at 22 °C in the absence of substrate. The experimental error of the measured deuteration levels is on the order of 1%.

Comparative measurements of thermolysin in the presence and absence of LeuEnk substrate were carried out using procedures similar to those described above. HCl (1.5 M) was used instead of phosphate buffer for quenching HDX at pH 2.5, and the pepsin stock solution had a concentration of 165 μM for a final thermolysin (and pepsin) concentration of 29 μM. Labeling solutions containing the reaction products Tyr-Gly-Gly and Phe-Leu were prepared by completely digesting 8.4 mM LeuEnk with 0.05 μM thermolysin in 100% D_2O buffer at room temperature overnight.

RESULTS AND DISCUSSION

Conformational Dynamics of Thermolysin in the Absence of Substrate. ESI-MS-based HDX experiments were initially carried out on thermolysin in the absence of substrate and at a temperature of 22 °C. Peptic digestion resulted in 41 fragments that were suitable for probing the isotope exchange behavior of the protein, corresponding to a sequence coverage of 99% (Figure 2). The HDX kinetics of the various peptides exhibit dramatic differences. For example, fragment 139−150 undergoes hardly any exchange during the experimental time window of 5 h (Figure 3A−E). A slow mass increase occurs for fragment 83−97 (Figure 3F−J), whereas intermediate HDX kinetics are seen for fragment 192−202 (Figure 3K−O), and faster kinetics for fragment 41−54 (Figure 3P−T). Fragment 13−19 shows a pronounced labeling burst phase for the earliest observation time (14 s) and virtually no change thereafter (Figure 3U−Y). No other peptide showed this particular type of behavior. A more complete view of the spatially resolved HDX kinetics is provided in Figure 4, which summarizes data for 22 peptides that cover almost the entire protein sequence.

The observation of gradual mass shifts without peak splitting implies that HDX occurs in the EX2 regime (*19*).

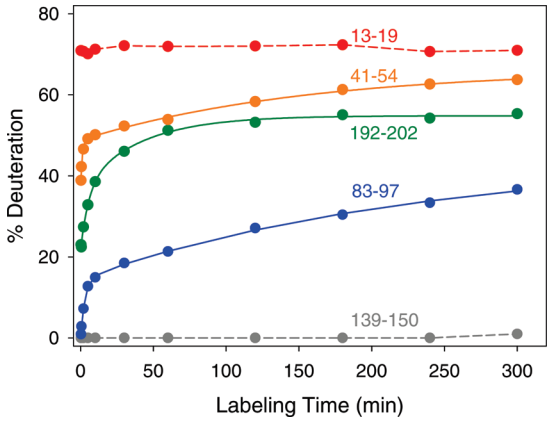

FIGURE 5: Deuteration kinetics of the five peptic fragments from Figure 3. Solid lines for 83−97, 192−202, and 41−54 represent biexponential fits, as described in the text. Dashed lines for 13−19 and 139−150 are for illustrative purposes only. The color coding follows the classification defined in Figure 6.

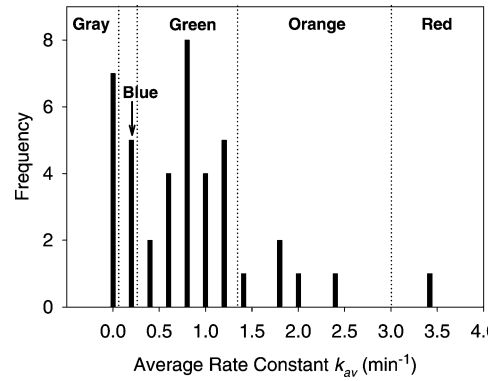

FIGURE 6: 18-Bin histogram generated from the average HDX rate constants k_{av} for 41 peptic fragments (22 °C, no substrate). Dashed lines indicate boundaries used to categorize the isotope exchange as slowest (gray), slow (blue), intermediate (green), fast (orange), and fastest (red).

Thus, the HDX rate constant at any given amide is given by $k_{HDX} = (k_{unfold}/k_{fold})k_{ch}$, where k_{unfold} and k_{fold} are residue-specific rate constants of the structural fluctuations that mediate exchange. Because the measurements were carried out in a native solvent environment, these dynamics are likely dominated by local and subglobal unfolding−refolding, whereas global transitions play a minor role (*20, 44*). The value of the chemical exchange rate constant k_{ch} is on the order of 20 s^{-1} for the conditions used here (*45*). EX2 measurements do not provide direct information on the time scale of structural fluctuations, other than $k_{fold} \gg k_{ch}$ (*18*).

Seven peptides do not show any appreciable HDX for labeling times up to 5 h. In addition to 139−150 (Figure 3), this group comprises 63−82, 63−75, 139−149, 139−151, 167−175, and 303−310. With the exception of these species, and the extremely rapidly exchanging peptide 13−19 (Figure 3), the labeling kinetics of all fragments are well described by a biexponential expression

$$D(t) = A_0 + A_1[1 - \exp(-k_1 t)] + A_2[1 - \exp(-k_2 t)] \quad (2)$$

where $D(t)$ is the deuteration level (expressed in percent), A_0 is the fraction of hydrogens that undergo burst phase exchange, and A_1 and A_2 are the fractions that are labeled with k_{HDX} rate constants k_1 and k_2, respectively. When averaging the data for all peptides, the mean values of the two rate constants are $\bar{k}_1 = 0.46$ min^{-1} and $\bar{k}_2 = 0.013$ min^{-1}. The fraction of hydrogens that appear unexchangeable during the 5 h experimental time window is given by

$$A_3 = 100\% - (A_0 + A_1 + A_2) \quad (3)$$

Examples of fits obtained in this way are depicted for fragments 83−97, 192−202, and 41−54 in Figure 5. For discussing the measured kinetics it is convenient to characterize the behavior of every single peptide by a single parameter. For this purpose, average rate constants k_{av} were calculated for each fragment according to

$$k_{av} = (10A_0\bar{k}_1 + A_1k_1 + A_2k_2 + 0.1A_3\bar{k}_2)/100 \quad (4)$$

For this calculation it was arbitrarily assumed that burst-phase labeling (A_0) proceeds with a rate constant equal to ten times $\bar{k}_1$ and that the slowest exchange events (A_3) occur with $0.1\bar{k}_2$. For peptides with "flat" exchange profiles (e.g., 13−19, 139−150) k_{av} was calculated on the basis of the corresponding A_0 and A_3 values only. The average rate constants obtained from eq 4 span a range from 0.0013 to 3.3 min^{-1}. On the basis of a histogram of all the values obtained (Figure 6) the exchange kinetics of individual peptides were divided into five categories, i.e., slowest (k_{av} < 0.002 min^{-1}), slow (0.002 min^{-1} < k_{av} < 0.2 min^{-1}), intermediate (0.2 min^{-1} < k_{av} < 1.4 min^{-1}), fast (1.4 min^{-1} < k_{av} < 3 min^{-1}), and fastest (k_{av} > 3 min^{-1}). The colors gray, blue, green, orange, and red, respectively, were assigned to these five groups. A backbone representation of thermolysin using this color scheme is depicted in Figure 7. The same color scheme was used in Figures 2 and 5.

Interpretation of HDX Data for Substrate-Free Thermolysin. The fastest exchanging, and hence the most mobile, regions of the protein are located in the periphery of the two lobes, i.e., residues 1−27 and 41−54 in the N-terminal half and residues 244−254 in the C-terminal section (Figures 2, 4, and 7). These areas comprise several extensive loops that undergo marked structural changes upon substrate binding according to a comparison of the corresponding X-ray structures (*29, 30*).

It is striking that the hinge region with the active site cleft exhibits relatively slow HDX kinetics. Three of the active site residues are in sections that undergo very slow exchange (gray), including the Zn^{2+} ligands His142 and His146. The third ligand Glu166 is part of the "green" peptide 156−166; however, it is located directly adjacent to a "gray" area (167−175, Figures 2 and 4). This positioning makes it likely that the conformational flexibility of Glu166 is also very limited. These observations imply that the three Zn^{2+}-coordinating residues form a fairly immobile scaffold, which allows the metal ion to act as a firm pivot point during catalysis. Six of the other active site amino acids exhibit an intermediate ("green") degree of conformational flexibility. Despite the undeniable importance of enzyme structural dynamics (*1–6, 34, 36, 46–49*), our data indicate that the residues in the active site of thermolysin are only moderately flexible, even containing elements that exhibit considerable stiffness. These findings suggest that a certain degree of rigidity in the catalytic cleft may be required to ensure specificity during substrate binding, along with a suitable prepositioning of active site residues. At the same time, there has to be some flexibility to allow individual side chains to adopt their catalytically active orientations during hinge

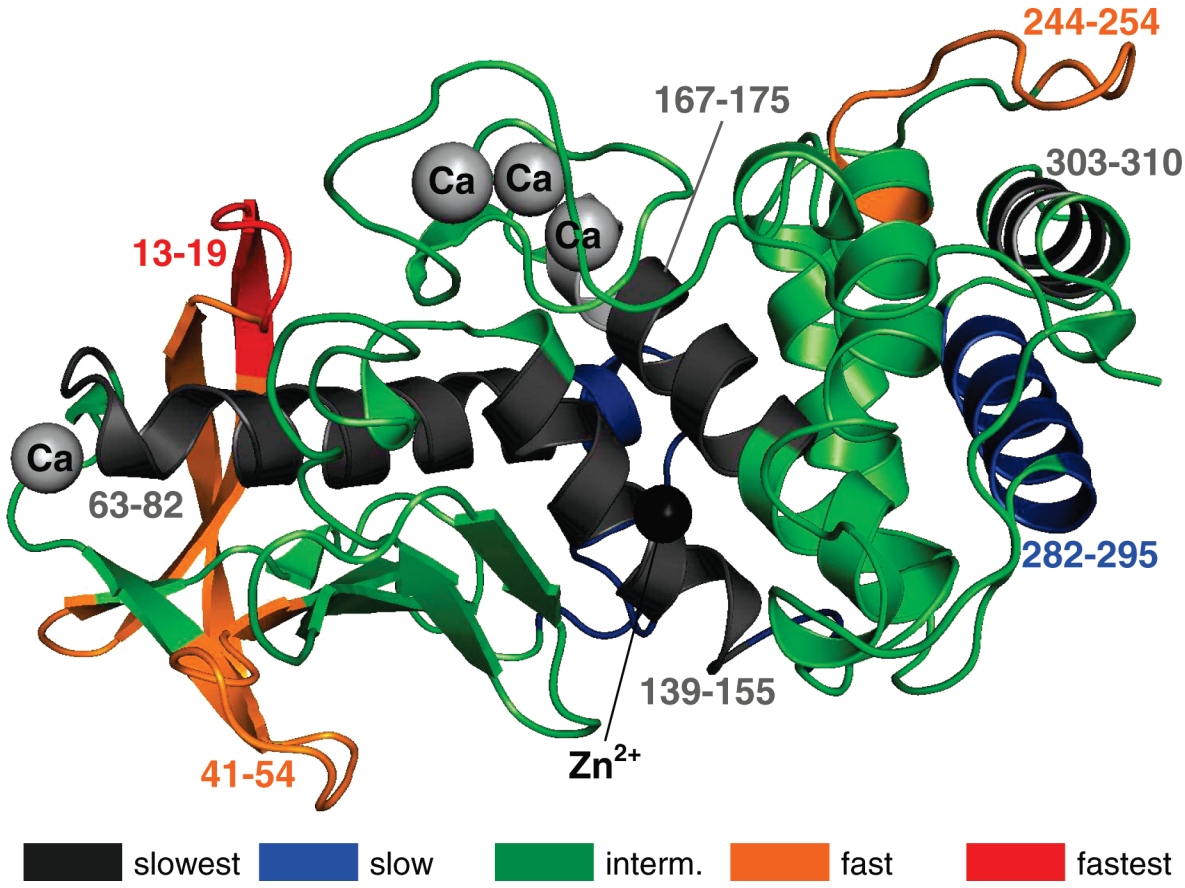

FIGURE 7: Structure of thermolysin shown in the same orientation as in Figure 1. The backbone is colored to reflect the HDX kinetics of individual segments, using the color scheme of Figure 6. A few segments are identified by their residue numbers.

bending. The absence of very rapidly exchanging (and hence partially unfolded) regions in the active site could be required for efficient product release following the catalytic step, since disordered elements might lead to nonspecific binding. Overall, the presence of both rigid and moderately flexible elements in the active site of thermolysin may reflect a carefully tuned balance that is a prerequisite for function.

Turnover Kinetics. LeuEnk (Tyr-Gly-Gly-Phe-Leu) is a commonly used test substrate of thermolysin, with K_M = 0.2 mM and k_{cat} = 160 s^{-1} (*50*). This peptide is cleaved into Tyr-Gly-Gly and Phe-Leu, none of which is further hydrolyzed to any significant extent. A few details need to be addressed prior to discussing comparative thermolysin HDX experiments in the presence and absence of this substrate.

Enzyme kinetic studies typically monitor substrate depletion or product formation under saturating steady-state conditions. For these measurements the reaction rate can be freely adjusted by lowering the enzyme concentration down to the nanomolar range (or lower), such that the process occurs on a conveniently slow time scale. HDX/ESI-MS, however, monitors the enzyme itself (not the substrate or product) and thus requires a relatively high protein concentration. Such conditions tend to result in prohibitively large amounts of substrate. For example, 10 μM thermolysin would catalyze the conversion of almost 30 M LeuEnk during the 5 h time window that was used for the HDX measurements above. For the current work it was thus chosen to expose thermolysin to an easily manageable amount of LeuEnk, accepting the fact that enzyme activity can only be maintained for a brief time interval. The duration of this activity period was determined by monitoring substrate consumption

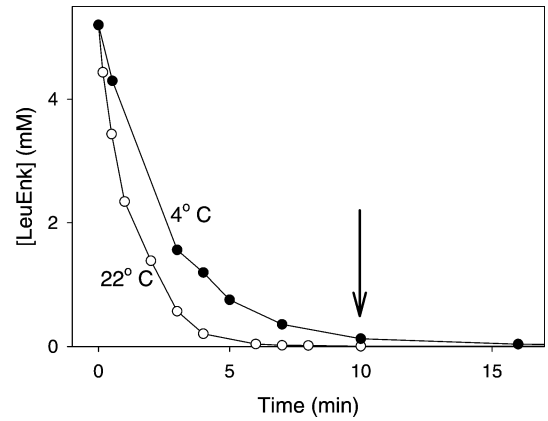

FIGURE 8: Kinetics of LeuEnk depletion at 4 and 22 °C at a thermolysin concentration of 0.5 μM. Measurements were conducted by removing aliquots from the reaction mixture at selected time points, followed by acid quenching at pH to 2.5 and flash freezing. The mixture was analyzed by ESI-MS following thawing and 3600-fold dilution in dilute aqueous acetic acid (pH 2.7) with 20% acetonitrile. Measured LeuEnk ion intensities were converted to concentration using a linear calibration plot that had been generated in separate control experiments (not shown). The arrow corresponds to the time point when virtually all of the substrate has been consumed at 4 °C.

for $[LeuEnk]_0$ = 5.2 mM at an enzyme concentration of 0.5 μM. The initial rate at 22 °C corresponds to k_{cat} = 160 s^{-1} (Figure 8, open symbols), which is consistent with the literature value (*50*). The reaction time can be extended by lowering the temperature to 4 °C, resulting in k_{cat} = 56 s^{-1}. Inspection of the time profile for T = 4 °C (Figure 8, solid symbols) reveals that complete substrate depletion requires

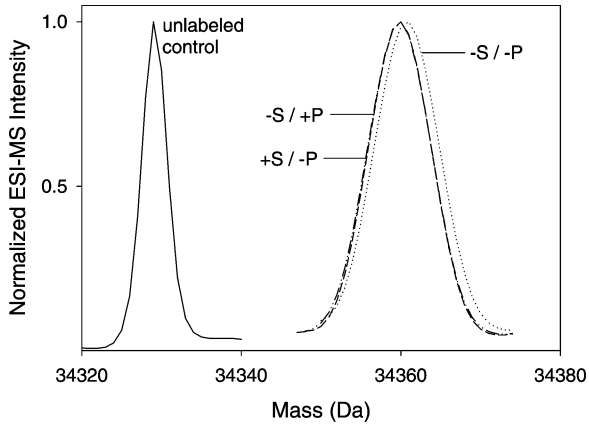

FIGURE 9: Deconvoluted ESI mass distributions of intact thermolysin after 10 s of HDX under different conditions: (−S/−P) without substrate and without product; (−S/+ P) without substrate but with product; (+S/−P) with substrate but without product. The spectrum of the unlabeled protein is shown for comparison (solid line).

ca. 10 min, as marked by the arrow (Figure 8). On the basis of this result it is possible to extrapolate to the conditions used for HDX/ESI-MS. LeuEnk and its hydrolysis products cause considerable signal suppression, thereby necessitating an increased thermolysin concentration of 38 μM. Substrate depletion under these conditions is complete after $t \approx 10$ s [calculated as 10 min × (0.5 μM/38 μM) × (6.7 mM/5.2 mM)] at 4 °C for $[\text{LeuEnk}]_0 = 6.7$ mM. Monitoring multiple time points during such a short interval is feasible in principle but remains technically challenging (*41, 51*). For the current work it was thus decided to base a comparison of the thermolysin HDX behavior on single time point measurements at $t = 10$ s and $T = 4$ °C.

Thermolysin can withstand temperatures up to 65 °C without inactivation, and it might be argued that the conditions used here are somewhat atypical for an enzyme isolated from a thermophilic organism. However, the data in Figure 8 clearly reveal that thermolysin is active at 4 °C, implying that all of the structural motions required for catalysis do occur under the conditions of this work. The approach of reducing the reaction rate by lowering the temperature to 4 °C, therefore, does not represent an impediment for studying the conformational dynamics of the protein.

Comparative HDX Measurements of Catalytically Active and Inactive Thermolysin. The conformational dynamics of thermolysin were compared at 4 °C in a 10 s time window under three different conditions; in the absence of both substrate and product (−S/−P), in the absence of substrate but with product (−S/+P), and in the presence of substrate without product (+S/−P). The term "product" refers to a mixture containing 6.7 mM of both hydrolysis products Tyr-Gly-Gly and Phe-Leu.

The first two conditions represent the resting state of the enzyme, where no catalysis takes place. Thermolysin shows slightly more extensive HDX for −S/−P than for −S/+P, corresponding to a difference of one to two deuterium atoms for the intact protein (Figure 9). This very small effect may be due to low affinity binding of the product to the protein, which can result in a marginal stabilization and possible steric shielding. Considerably larger HDX differences are generally observed for enzymes in the presence of high-affinity ligands (*41, 52*).

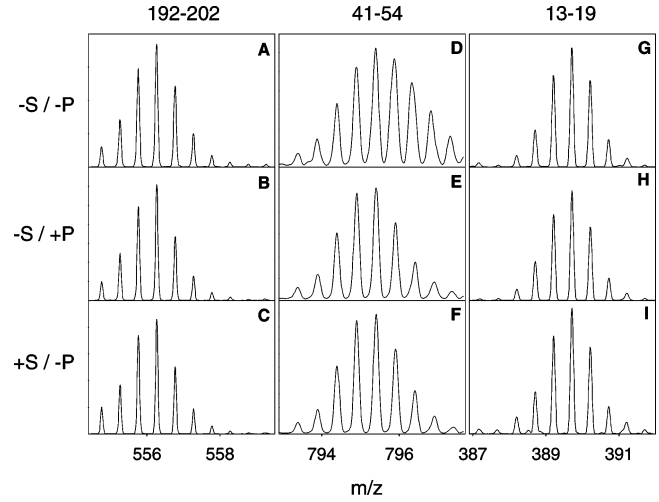

FIGURE 10: ESI mass spectra of three peptic fragments generated after 10 s of HDX under different conditions. The notation (−S/−P), (−S/+ P), and (+S/−P) is the same as in Figure 9. Panels: A−C, fragment 192−202; D−F, fragment 41−54; G−I, fragment 13−19.

The crucial question addressed in this study is whether the HDX behavior of thermolysin is different during catalysis and in the resting state. It is most suitable to contrast the conditions −S/+P versus +S/−P, because this ensures that the solvent environment in the two experiments is matched as closely as possible. No catalysis takes place for −S/+P. In contrast, under +S/−P conditions every enzyme molecule undergoes an average of 6.7 mM/38 μM = 176 catalytic turnover events which are accompanied by at least as many closing/opening hinge bending movements (*30*). Since not every enzyme−substrate encounter may result in a successful reaction, the actual number of closing/opening transitions performed by the catalytically active enzyme could be considerably higher. Strikingly, the HDX behavior of intact thermolysin under −S/+P and +S/−P conditions is identical, as seen from the mass distributions in Figure 9. It might be suspected that possible differences are masked by the occurrence of more rapid exchange in some protein regions that are compensated by slower HDX in other regions. However, peptide mapping reveals that this is not the case. The isotope exchange behavior for each of the 41 peptic fragments is indistinguishable, within experimental error, under −S/+P and +S/−P conditions. Raw data for three selected peptides are depicted in Figure 10, and a more complete overview is provided in Figure 11. Slightly elevated HDX levels are seen for some peptides under −S/−P conditions in Figure 11, as expected on the basis of the behavior of the intact protein (Figure 9). Nonetheless, the overall conclusion from the labeling data in Figures 9–11 is that the HDX properties of catalytically active and inactive thermolysin are indistinguishable.

CONCLUSIONS

HDX/ESI-MS for Monitoring Enzyme Dynamics. Short-term (10 s) isotope exchange measurements were used in this study for comparing the structural fluctuations of thermolysin in the presence and absence of substrate. Despite the limited duration of the time window, the spatially resolved HDX data in Figure 11 provide a very detailed view of the protein's HDX properties, with deuteration levels

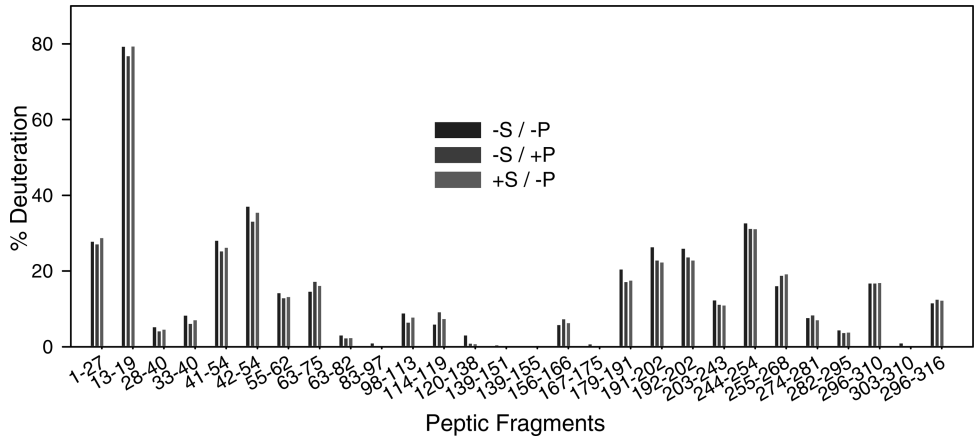

FIGURE 11: Deuteration levels of selected peptic fragments after 10 s of HDX under different conditions. The notation is the same as in Figure 9. The experimental error of the measured deuteration levels is on the order of 1%.

ranging from close to 0 to almost 80% (Figure 11). With the exception of highly protected ("blue" and "gray") regions, a ranking of peptides based on their k_{av} values is consistent with the HDX levels observed after short-term labeling. Clearly, any major changes in the conformational dynamics of thermolysin should be easily recognizable from the short-term labeling data of Figures 9–11. Previous NMR experiments were able to monitor enzymes under turnover conditions for much longer times by resorting to measurements on equilibrium systems, where the reaction flux in both directions is the same (*37*). While such an approach is very elegant, it represents a somewhat specialized scenario. For example, it is not clear if turnover under those conditions always involves genuine substrate binding and product release steps. Instead, substrate/product molecules might undergo cyclic interconversion without leaving the vicinity of the active site. The thermolysin-catalyzed hydrolysis of LeuEnk studied here represents the more typical case of a reaction far from equilibrium that is practically unidirectional.

HDX/ESI-MS monitors isotope exchange that is mediated by short-lived unfolding−refolding events linked to the transient disruption of hydrogen bonds. Every protein undergoes conformational dynamics of this type on a wide range of time scales (*18*). During catalysis thermolysin undergoes closing/opening hinge bending movements, in addition to structural changes in the periphery of the two lobes (*29, 30*). It is important to note that these functional motions are not directly equivalent to the unfolding−refolding transitions that mediate HDX. Nonetheless, both types of dynamics should be correlated (*10*), because localized rapid fluctuations appear to be directly linked to more extensive conformational switching events that occur on slower time scales (*40, 53, 54*). Thus, the occurrence of drastically different large-scale motions with and without substrate should lead to marked alterations in the HDX behavior. Changes would be expected to be most prevalent in the hinge region of thermolysin, comprising the "gray" sections 139−155 and 167−175, as well as the "green" 179−202 loops which bind three calcium ions (Figure 7). Other likely candidates include the highly mobile "orange" and "red" sections in the periphery of the two lobes, which also undergo structural changes during closing/opening of the enzyme (*29, 30*). Intriguingly, every single peptic fragment of thermolysin exhibits HDX characteristics that are indistinguishable under +S/−P and −S/+P conditions. It is concluded that the structural dynamics of the enzyme are very much alike during catalysis and in the absence of substrate. This finding is compatible with the idea that hinge bending and other catalytically relevant motions are sampled by the protein regardless of whether substrate turnover takes place or not. The view emerging from these thermolysin experiments and from recent NMR data on other proteins (*31, 37, 55*) is that catalytically relevant motions preexist in the substrate-free state. Hence, substrate turnover appears to be limited by the *intrinsic* dynamics of the protein.

Two Different Views of Enzyme Action. While considerable progress is being made in deciphering bioorganic aspects of enzymatic reaction mechanisms, the relationship between catalysis and protein dynamics remains poorly understood. One might consider two limiting scenarios for a hinge-bending enzyme, where functionally required motions occur in a stochastic or in a deterministic fashion. In the former case, it can be envisioned that a free enzyme undergoes random fluctuations that lead to the transient population of mechanistically relevant conformers. Addition of substrate in this scenario does not change the character of the dynamics considerably. Even substrate binding to the active site has little consequence; in particular, the substrate does *not* induce a transition to the closed state. Instead, the functionally required switch to the closed conformer is a random event that can occur regardless of whether substrate is present or not. In the absence of a suitable closing event the enzyme−substrate encounter will not result in successful turnover, and the unmodified substrate will dissociate from the active site. The opposite of this concept is a strictly deterministic model where the substrate induces changes of the overall energy landscape, forcing the protein along a specific conformational trajectory that culminates in turnover. Specifically, the energy release associated with binding is channeled into a major structural transition to the closed state, from which successful conversion to the product ensues. Once the product has been formed, the catalytic cycle is completed by triggering an opening transition. Catalysis in this second case involves protein motions that do not occur in the absence of substrate, and therefore, the overall conformational dynamics should be very different during catalysis and for the free enzyme.

These two hypothetical scenarios represent extreme cases, and it might be expected that "real" enzyme mechanisms involve both stochastic and deterministic elements. The HDX

data presented in this work reveal that the conformational dynamics of thermolysin during catalysis and without substrate are very much alike. This finding supports the notion that conformational transitions associated with catalysis follow a pattern that is predominantly stochastic. It will be interesting to see if future studies on other types of enzymes and different enzyme/substrate combinations will come to similar conclusions.

REFERENCES

1. Hammes, G. G. (2002) Multiple conformational changes in enzyme catalysis. *Biochemistry 41*, 8221–8228.
2. Benkovic, S. J., and Hammes-Schiffer, S. (2006) Enzyme Motions Inside and Out. *Science 312*, 208–209.
3. Daniel, R. M., Dunn, R. V., Finney, J. L., and Smith, J. C. (2003) The Role of Dynamics in Enzyme Activity. *Annu. Rev. Biophys. Biomol. Struct. 32*, 69–92.
4. Agarwal, P. A. (2006) Enzymes: An integrated view of structure, dynamics and function. *Microb. Cell Fact. 5*, 1–12.
5. Boehr, D. D., McElheny, D., Dyson, H. J., and Wright, P. E. (2006) The Dynamic Energy Landscape of Dihydrofolate Reductase Catalysis. *Science 313*, 1638–1642.
6. Pu, J., and Karplus, M. (2008) How subunit coupling produces the γ-subunit rotary motion in F_1-ATPase. *Proc. Natl. Acad. Sci. U.S.A. 105*, 1192–1197.
7. Yon, J., Perahia, D., and Ghelis, C. (1998) Conformational dynamics and enzyme activity. *Biochimie 80*, 33–42.
8. Liang, Z.-X., Lee, T., Resing, K. A., Ahn, N. G., and Klinman, J. P. (2004) Thermal-activated protein mobility and its correlation with catalysis in thermophilic alcohol dehydrogenase. *Proc. Natl. Acad. Sci. U.S.A. 101*, 9556–9561.
9. Sola, R. J., and Griebenow, K. (2006) Chemical glycosylation: New Insights on the interrelation between protein structural mobility, thermodynamic stability, and catalysis. *FEBS Lett. 580*, 1685–1690.
10. Codreanu, S. G., Ladner, J. E., Xiao, G., Stourman, N. V., Hachey, D. L., Gilliland, G. L., and Armstrong, R. N. (2002) Local Protein Dynamics and Catalysis: Detection of Segmental Motion Associated with Rate-Limiting Product Release by a Glutathione Transferase. *Biochemistry 41*, 15161–15172.
11. Falzone, C. J., Wright, P. E., and Benkovic, S. J. (1994) Dynamics of a Flexible Loop in Dihydrofolate Reductase from *Escherichia coli* and Its Implications for Catalysis. *Biochemistry 33*, 439–442.
12. Cole, R., and Loria, J. P. (2002) Evidence for Flexibility in the Function of Ribonuclease A. *Biochemistry 41*, 6072–6081.
13. Eisenmesser, E. Z., Bosco, D. A., Akke, M., and Kern, D. (2002) Enzyme Dynamics During Catalysis. *Science 295*, 1520–1523.
14. Wand, A. J. (2001) Dynamic activation of protein function: A view emerging from NMR spectroscopy. *Nat. Struct. Biol. 8*, 926–931.
15. Busenlehner, L. S., Salomonsson, L., Brzezinski, P., and Armstrong, R. N. (2006) Mapping protein dynamics in catalytic intermediates of the redox-driven proton pump cytochrome c oxidase. *Proc. Natl. Acad. Sci. U.S.A. 103*, 15398–15403.
16. Case, D. A. (2002) Molecular Dynamics and NMR Spin Relaxation in Proteins. *Acc. Chem. Res. 35*, 325–331.
17. Hvidt, A., and Nielsen, S. O. (1966) Hydrogen exchange in proteins. *Adv. Protein Chem. 21*, 287–386.
18. Krishna, M. M. G., Hoang, L., Lin, Y., and Englander, S. W. (2004) Hydrogen exchange methods to study protein folding. *Methods 34*, 51–64.
19. Miranker, A., Robinson, C. V., Radford, S. E., and Dobson, C. M. (1996) Investigation of protein folding by mass spectrometry. *FASEB J. 10*, 93–101.
20. Bai, Y., Sosnick, T. R., Mayne, L., and Englander, S. W. (1995) Protein Folding Intermediates: Native State Hydrogen Exchange. *Science 269*, 192–197.
21. Smith, D. L., Deng, Y., and Zhang, Z. (1997) Probing the noncovalent structure of proteins by amide hydrogen exchange mass spectrometry. *J. Mass Spectrom. 32*, 135–146.
22. Wales, T. E., and Engen, J. R. (2006) Hydrogen Exchange Mass Spectrometry for the Analysis of Protein Dynamics. *Mass Spectrom. Rev. 25*, 158–170.
23. Englander, S. W. (2006) Hydrogen Exchange and Mass Spectrometry: A Historical Perspective. *J. Am. Soc. Mass Spectrom. 17*, 1481–1489.
24. Pantazatos, D., Kim, J. S., Klock, H. E., Stevens, R. C., Wilson, I. A., Lelsey, S. A., and Woods, V. L. (2004) Rapid refinement of crystallographic protein construct definition employing enhanced hydrogen/deuterium exchange MS. *Proc. Natl. Acad. Sci. U.S.A. 101*, 751–756.
25. Lu, X., Wintrode, P. L., and Surewicz, W. K. (2007) β-Sheet core of human prion protein amyloid fibrils as determined by hydrogen/deuterium exchange. *Proc. Natl. Acad. Sci. U.S.A. 104*, 1510–1515.
26. Yan, X., Zhang, H., Watson, J., Schimerlik, M. I., and Deinzer, M. L. (2002) Hydrogen/deuterium exchange and mass spectrometric analysis of a protein containing multiple disulfide bonds: Solution structure of recombinant macrophage colony stimulating factor-beta (rhM-CSFβ). *Protein Sci. 11*, 2113–2124.
27. Matthews, B. W. (1988) Structural Basis of the Action of Thermolysin and Related Zinc Peptidases. *Acc. Chem. Res. 21*, 333–340.
28. Juers, D. H., Kim, J., Matthews, B. W., and Sieburth, S. M. (2005) Structural Analysis of Silanediols as Transition-State-Analogue Inhibitors of the Benchmark Metalloprotease Thermolysin. *Biochemistry 44*, 16524–16528.
29. Holland, D. R., Tronrud, D. E., Pley, H. W., Flaherty, K. M., Stark, W., Jansonius, J. N., McKay, D. B., and Matthews, B. W. (1992) Structural comparison suggests that thermolysin and related neutral proteases undergo hinge-bending motion during catalysis. *Biochemistry 31*, 11310–11316.
30. Hausrath, A. C., and Matthews, B. W. (2002) Thermolysin in the absence of substrate has an open conformation. *Acta Crystallogr. D 58*, 1002–1007.
31. Vendruscolo, M., and Dobson, C. M. (2006) Dynamic Visions of Enzymatic Reactions. *Science 313*, 1586–1587.
32. Radkiewicz, J. L., and Brooks, C. L. (2000) Protein Dynamics in Enzymatic Catalysis: Exploration of Dihydrofolate Reductase. *J. Am. Chem. Soc. 122*, 225–231.
33. Sawaya, M. R., and Kraut, J. (1997) Loop and Subdomain movements in the Mechanism of *Escherichia coli* Dihydrofolate Reductase: Crystallographic Evidence. *Biochemistry 36*, 586–603.
34. Falke, J. J. (2002) A Moving Story. *Science 295*, 1480–1481.
35. Agarwal, P. A., Geist, A., and Gorin, A. (2004) Protein Dynamics and Enzymatic Catalysis: Investigating the Peptidyl-Prolyl Cis-Trans Isomerization Activity of Cyclosporin A. *Biochemistry 43*, 10605–10618.
36. Huang, Y. J., and Montelione, G. T. (2005) Proteins flex to function. *Nature 438*, 36–37.
37. Eisenmesser, E. Z., Miller, O., Labeikovsky, W., Korzhnev, D. M., Wolf-Watz, M., Sosco, D. A., Skalicky, J. J., Kay, L. E., and Kern, D. (2005) Intrinsic dynamics of an enzyme underlies catalysis. *Nature 438*, 117–121.
38. Resing, K. A., and Ahn, N. G. (1998) Deuterium Exchange Mass Spectrometry as a Probe of Protein Kinase Activation. Analysis of Wild-Type and Constitutively Active Mutants of MAP Kinase Kinase-1. *Biochemistry 37*, 463–475.
39. Agarwal, P. A. (2005) Role of Protein Dynamics in Reaction Rate Enhancement by Enzymes. *J. Am. Chem. Soc. 127*, 15248–15256.
40. Henzler-Wildman, K. A., Lei, M., Thai, V., Kerns, S. J., Karplus, M., and Kern, D. (2007) A hierarchy of timescales in protein dynamics is linked to enzyme catalysis. *Nature 450*, 913–918.
41. Liu, Y.-H., and Konermann, L. (2006) Enzyme conformational dynamics during catalysis and in the "resting state" monitored by hydrogen/deuterium exchange mass spectrometry. *FEBS Lett. 580*, 5137–5142.
42. O'Donohue, M. J., Roques, B. P., and Beaumont, A. (1994) Cloning and expression in *Bacillus subtilis* of the npr gene from *Bacillus thermoproteolyticus* rokko coding for the thermostable metalloprotease thermolysin. *Biochem. J. 300*, 599–603.
43. Weis, D. D., Engen, J. R., and Kass, I. J. (2006) Semi-Automated Data Processing of Hydrogen Exchange Mass Spectra Using *HX-EXPress*. *J. Am. Soc. Mass Spectrom. 17*, 1700–1703.
44. Maity, H., Lim, W. K., Rumbley, J. N., and Englander, S. W. (2003) Protein hydrogen exchange mechanism: Local fluctuations. *Protein Sci. 12*, 153–160.
45. Bai, Y., Milne, J. S., Mayne, L., and Englander, S. W. (1993) Primary Structure Effects on Peptide Group Hydrogen Exchange. *Proteins: Struct., Funct., Genet. 17*, 75–86.
46. Gao, J. (2003) Catalysis by enzyme conformational change as illustrated by orotidine 5′-monophosphate decarboxylase. *Curr. Opin. Struct. Biol. 13*, 184–192.
47. Benkovic, S. J., and Hammes-Schiffer, S. (2003) A Perspective on Enzyme Catalysis. *Science 301*, 1196–1202.

48. Garcia-Viloca, M., Gao, J., Karplus, M., and Truhlar, D. G. (2004) How Enzymes Work: Analysis by Modern Rate theory and Computer Simulations. *Science 303*, 186–195.
49. Cannon, W. R., Singleton, S. F., and Benkovic, S. J. (1996) A perspective on biological catalysis. *Nat. Struct. Biol. 3*, 821–833.
50. Marie-Claire, C., Ruffet, E., Antonczak, S., Beaumont, A., O'Donohue, M., Roques, B. P., and Fournie-Zaluski, M.-C. (1997) Evidence by Site-Directed Mutagenesis That Arginine 203 of Thermolysin and Arginine 717 of Neprilysin (Neutral Endopeptidase) Play Equivalent Critical Roles in Substrate Hydrolysis and Inhibitor Binding. *Biochemistry 36*, 13938–13945.
51. Rist, W., Rodriguez, F., Jorgensen, T. J. D., and Mayer, M. P. (2005) Analysis of subsecond protein dynamics by amide hydrogen exchange and mass spectrometry using a quench-flow setup. *Protein Sci. 14*, 626–632.
52. King, D., Bergmann, C., Orlando, R., Benen, J. A. E., Kester, H. C. M., and Visser, J. (2002) Use of Amide Exchange Mass Spectrometry To Study Conformational Changes within the Endopolygalacturonase II-Homogalacturonan-Polygalacturonase Inhibiting Protein System. *Biochemistry 41*, 10225–10233.
53. Döring, K., Surrey, T., Grunewald, S., John, E., and Jähnig, F. (2000) Enhanced internal dynamics of a membrane transport protein during substrate translocation. *Protein Sci. 9*, 2246–2250.
54. Simmons, D. A., Dunn, S. D., and Konermann, L. (2003) Conformational Dynamics of Partially Denatured Myoglobin Studied by Time-Resolved Electrospray Mass Spectrometry with Online Hydrogen-Deuterium Exchange. *Biochemistry 42*, 5896–5905.
55. Henzler-Wildman, K. A., Thai, V., Lei, M., Ott, M., Wolf-Watz, M., Fenn, T., Pozharski, E., Wilson, A. M., Petsko, A. G., Karplus, M., Hübner, C. G., and Kern, D. (2007) Intrinsic motions along an enzymatic reaction trajectory. *Nature 450*, 838–844.

BI800463Q